Low voltage and high transmittance blue-phase liquid crystal displays with corrugated electrodes

Meizi Jiao, Yan Li, and Shin-Tson Wu[a)]
College of Optics and Photonics, University of Central Florida, Orlando, Florida 32816, USA

(Received 29 November 2009; accepted 16 December 2009; published online 4 January 2010)

A low voltage (<10 V) and high transmittance (~85.6%) polymer-stabilized blue-phase liquid crystal (BPLC) display is proposed. The periodic corrugated electrodes generate a strong horizontal field component to induce isotropic-to-anisotropic transition in the BPLC medium through Kerr effect. Moreover, this field is uniformly distributed across the entire LC layer so that the accumulated phase retardation along the beam path is large, resulting in low voltage and high transmittance. This approach enables BPLC to be addressed by amorphous-silicon thin film transistors, which would accelerate its emergence as next-wave display technology. © *2010 American Institute of Physics*. [doi:10.1063/1.3290253]

Polymer-stabilized blue phase liquid crystal (PS-BPLC) (Refs. 1–3) is emerging as a next-generation display technology because of its revolutionary features, such as submillisecond response time which is ~10× faster than a typical nematic, no need for alignment layer, and inherently wide viewing angle. Unlike a nematic LC which is based on anisotropic-to-anisotropic molecular reorientation, the physical mechanism of BPLC is governed by the Kerr effect-induced isotropic-to-anisotropic transition.[4–7] Fast response time enables color sequential displays using red, green, and blue LED backlight unit without noticeable color breakup. By eliminating spatial color filters, device resolution is tripled and optical efficiency improved by ~3×. However, two major technical challenges: high operating voltage (~50 V_{rms}) and relatively low transmittance (~65%) need to be overcome before widespread applications can take off.

Several approaches have been proposed to lower the operation voltage. For instance, a BPLC material with a large Kerr constant ($K \sim 12.7\ \mathrm{nm/V^2}$) (Ref. 8) has been recently developed to reduce the driving voltage from over 100 to ~50 V_{rms}. By optimizing the in-plane switching (IPS) electrode width and gap,[9,10] the operating voltage is further reduced to ~35 V_{rms}. However, these voltages are still far beyond the acceptable range of mainstream amorphous-silicon thin film transistors. Although some structures such as wall-shaped[11] and protrusion[12] electrodes show very positive trend to lower the driving voltage to 10 V_{rms}, the transmittance is sacrificed and moreover the device fabrication is rather difficult. Therefore, there is an urgent need to develop approaches for not only lowering the operation voltage but also keeping a high transmittance.

In this letter, we propose a device structure consisting of periodic corrugated electrodes which generates a strong horizontal electric field component and more importantly this field penetrates deeply into the LC medium. These two factors jointly contribute to reduce the operation voltage to below 10 V. Meanwhile, the electric field generated by such a structure is uniformly distributed across the entire pixel area and this plays a crucial role for obtaining high transmittance (~85%).

Figure 1 depicts the device structure of our proposed electrode configuration. The BPLC cell is sandwiched between two crossed polarizers, thus, it is a normally black display. A biaxial compensation film is used to widen the viewing angle. Both top and bottom substrates are fabricated with periodic corrugated structures. As compared to typical dimensions of patterned IPS electrodes, the electrode period W in our structure is quite large. As an example, in our simulations we choose $W=40\ \mu\mathrm{m}$ and the inclination angle of the corrugations $\alpha=60°$. These dimensions are similar to those of backlight films such as turning film,[13] and can be fabricated fairly easily by mold-pressing method or printing method. In each pixel, the common electrodes are coated over the entire top substrate without patterning and the pixel electrodes coated on bottom substrate. In practice, all sharp edges drawn in Fig. 1 can be round and smooth to make fabrication easier. In our simulation, for simplicity we assume the corrugation has triangular shape. Performance will not be affected much because these edges happen to be dead zones with almost no transmittance. A BPLC with $K \sim 12.7\ \mathrm{nm/V^2}$ is assumed. The cell gap is 3.5 μm, but since the cell is tilted in vertical zigzags, the effective distance for normal incident light passing through the LC layer is $d/\cos(\alpha)$, which is 7 μm in our example.

In our numerical model, we assume BPLC is optically isotropic in the voltage-off state and compute the potential distribution by solving Poisson equation $\nabla(\nabla \cdot \varepsilon \Phi)=0$ and then the distribution of electric field $\boldsymbol{E}$. Based on the obtained electric field distribution, we calculate the induced

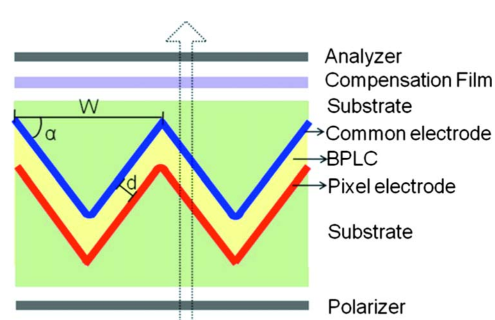

FIG. 1. (Color online) Cross-section view of proposed PS-BPLCD structure with corrugated driving electrodes.

a)Electronic mail: swu@mail.ucf.edu.

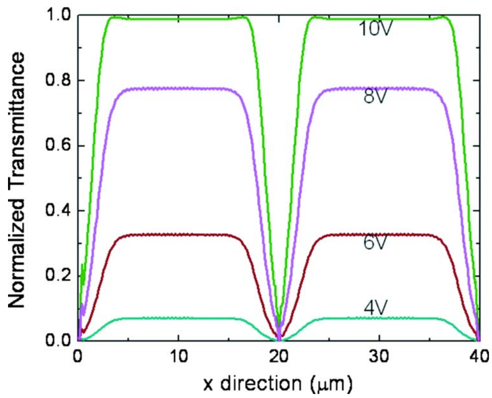

FIG. 2. (Color online) Simulated transmittance profile across an electrode period area at different driving voltages. Here the electrode period is 40 μm and λ=550 nm.

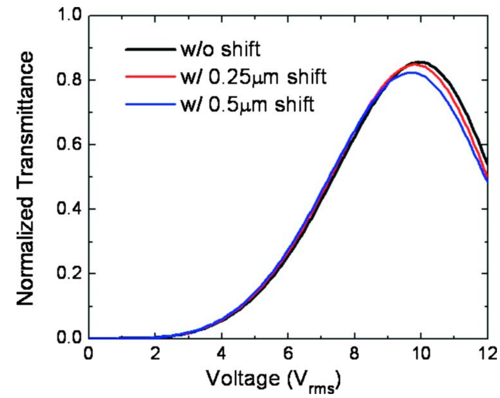

FIG. 3. (Color online) Normalized VT curves at λ=550 nm of the proposed PS-BPLCD under normal incidence (black curve). Red curve is VT curve with 0.25 μm horizontal shift between top and bottom electrodes and blue one with 0.5 μm shift.

birefringence Δn_{ind} from the following Kerr effect:[7,9]

$$\Delta n_{\text{ind}} = \lambda K E^2 = (\Delta n)_o (E/E_s)^2, \tag{1}$$

where λ is the incident light wavelength, K is the Kerr constant, $(\Delta n)_o$ is the maximum induced birefringence, and E_s is the saturation field. In Eq. (1), Kerr effect holds in the low field regime. As the electric field keeps increasing, the induced birefringence will gradually saturate but it cannot exceed the intrinsic birefringence of the LC/polymer composite when all the LC directors are eventually reoriented by the external field. Afterwards, we use extended Jones matrix[14] to calculate the electro-optical properties.

Figure 2 depicts the simulated transmittance ($\lambda = 550$ nm) of the BPLC cell at a cross-section along horizontal (x-axis) direction and some indicated voltages. The transmittance is normalized to that of two parallel polarizers (35%). Although the induced birefringence below 10 V_{rms} is still small and the optic axis is not completely orientated in the desired horizontal direction, its horizontal component is reasonably large. Furthermore, the induced birefringence is uniformly distributed inside the whole cell (z-axis) except at the turning edge areas, so the phase retardation can be accumulated along the entire traveling distance inside the LC layer. As a result, the on-state voltage is substantially reduced. As shown in Fig. 2, some transmission dead zones are found at every turning edge area. This is because the induced birefringence is along the vertical direction so that it makes no contribution to phase retardation. However, our electrodes are quite wide, thus the area ratio of these dead zones is relatively small. We could reduce this area ratio further by using a wider electrode. In comparison to IPS or wall-shaped electrodes,[10–12] our design exhibits a higher transmittance.

Figure 3 shows the normalized voltage-dependent transmittance (VT) curves of our device at λ=550 nm, as the black curve shows. With the parameters mentioned before, the on-state voltage occurs at $V_{\text{on}} \sim 9.9$ V_{rms} and the peak transmittance reaches 85.6%. The distance between the top and bottom electrodes, i.e., the LC cell gap is controlled by spacers, so its assembly error with current fabrication technology is small, usually below 0.3 μm. The horizontal alignment accuracy between top and bottom electrodes of our structure is also determined by spacers, so the assembly error is expected to be as small as cell gap variation. Here we plot in Fig. 3 are VT curves with 0.25 and 0.50 μm shift in horizontal direction between the top and bottom electrodes. It shows our structure is reasonably tolerant to assembly errors. With 0.25 μm misalignment, the shift in VT curve is almost unnoticeable. As misalignment increases to 0.50 μm, V_{on} drops to 9.7 V_{rms} and transmittance to 82.4%. From Fig. 3, the VT curves overlap with each other very well when $V < 9$ V_{rms}, which means this device is insensitive to horizontal shift if the device is driven below 9 V_{rms} where the transmittance maintains at ~80%.

Varying the device dimension will undoubtedly alter the electro-optical performance. Generally speaking, increasing the inclination angle of the corrugated electrodes helps to reduce the operation voltage. With a larger inclination angle, the horizontal component of the induced birefringence is enhanced and the effective path length of incident light inside LC medium is increased, so that the required phase retardation can be achieved with a lower voltage. A thinner cell gap is also helpful to reduce operation voltage. As the cell gap decreases, on one hand the optical path length d_{opl} is decreased; but on the other hand the induced birefringence Δn_{ind} increases in quadratic manner due to the stronger electric field. So overall speaking, since phase retardation is proportional to $d_{\text{opl}}\Delta n_{\text{ind}}$, a lower driving voltage can result in the same phase retardation in a thinner cell gap. Moreover, the dead zones become narrower in a thinner cell and thus transmittance will be improved. We summarize in Table I the driving voltage and transmittance in several examples with different inclination angles and cell gaps; here the electrode width is kept at 40 μm in all these examples. We monitor the induced birefringence during these calculations. The induced birefringence at effective areas is far below the saturation value, thus the Kerr effect is valid. From material viewpoint, a BPLC with a larger Kerr constant is always helpful for lowering the operation voltage.

TABLE I. On-state driving voltage (V_{on}) and corresponding transmittance (T) of the proposed PS-BPLCD with different electrode inclination angles (α) and LC cell gaps (d).

α (°)	d (μm)	V_{on} (V_{rms})	T (%)
45	3.5	14.9	86.3
75	3.5	6.2	84.7
60	2	7.5	93.4
60	5	12.1	80.5

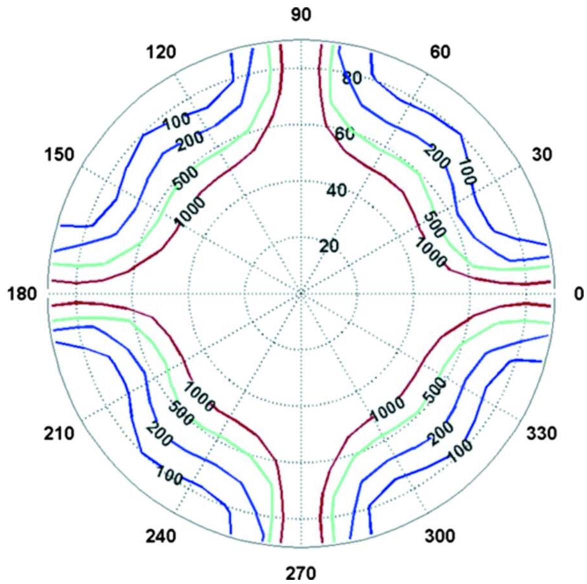

FIG. 4. (Color online) Simulated isocontrast plot of the proposed PS-BPLCD at $\lambda=550$ nm with one biaxial phase compensation film.

Wide view is another advantage of BP LCD. Macroscopically, BPLC is optically isotropic in the voltage-off state. Under such a circumstance, the light leakage at dark state is only from the crossed linear polarizers. Thus, the contrast ratio is expected to be high and viewing angle should be wide. Our structure has a zigzag shape in vertical direction, so two domains are automatically formed in the voltage-on state and this will further result in a symmetric viewing angle. Figure 4 shows the isocontrast contour of our device structure at $\lambda=550$ nm using one biaxial film[15] to compensate the light leakage at oblique angles. A half-wave biaxial film ($n_x=1.5110$, $n_y=1.5095$, $N_z=0.5$) can effectively compensate this mode and achieve a wide view. A contrast ratio larger than 100:1 can be obtained over 70° viewing cone.

In conclusion, the proposed corrugated electrode is effective for lowering the operating voltage and enhancing the transmittance of a blue phase LCD. Using a modest Kerr constant ($K\sim 12.7$ nm/V^2), the driving voltage is reduced to ~ 9.9 V_{rms}, which is $\sim 5\times$ lower than that employing conventional IPS electrodes, while keeping a high transmittance (85.6%). Besides low driving voltage and high transmittance, BPLC also exhibits wide viewing angle and fast response time. The latter enables color sequential displays, which will triple the device resolution and optical efficiency because of the elimination of color filters.

The authors are indebted to L. Rao for useful discussions and AFOSR for partial financial support under Contract No. FA95550-09-1-0170.

[1]H. Kikuchi, M. Yokota, Y. Hisakado, H. Yang, and T. Kajiyama, Nature Mater. **1**, 64 (2002).
[2]Y. Hisakado, H. Kikuchi, T. Nagamura, and T. Kajiyama, Adv. Mater. **17**, 96 (2005).
[3]S. W. Choi, S. I. Yamamoto, Y. Haseba, H. Higuchi, and H. Kikuchi, Appl. Phys. Lett. **92**, 043119 (2008).
[4]P. G. de Gennes and J. Prost, *The Physics of Liquid Crystals*, 2nd ed. (Clarendon, Oxford, 1993).
[5]S. Meiboom, J. P. Sethna, W. P. Anderson, and W. F. Brinkman, Phys. Rev. Lett. **46**, 1216 (1981).
[6]R. Memmer, Liq. Cryst. **27**, 533 (2000).
[7]J. Kerr, Philos. Mag. **50**, 337 (1875).
[8]H. Kikuchi, Y. Haseba, S. Yamamoto, T. Iwata, and H. Higuchi, SID Int. Symp. Digest Tech. Papers **40**, 578 (2009).
[9]Z. Ge, S. Gauza, M. Jiao, H. Xianyu, and S. T. Wu, Appl. Phys. Lett. **94**, 101104 (2009).
[10]Z. Ge, L. Rao, S. Gauza, and S. T. Wu, J. Disp. Technol. **5**, 250 (2009).
[11]M. Kim, M. S. Kim, B. G. Kang, M. K. Kim, S. Yoon, S. H. Lee, Z. Ge, L. Rao, S. Gauza, and S. T. Wu, J. Phys. D **42**, 235502 (2009).
[12]L. Rao, Z. Ge, S. T. Wu, and S. H. Lee, Appl. Phys. Lett. **95**, 231101 (2009).
[13]M. Oe and I. Chiba, U.S. Patent No. 5711589 (27 January 1998).
[14]Z. Ge, X. Zhu, T. X. Wu, and S. T. Wu, J. Opt. Soc. Am. A Opt. Image Sci. Vis. **22**, 966 (2005).
[15]M. Jiao, Z. Ge, and S. T. Wu, J. Disp. Technol. **5**, 331 (2009).